

Mechanistic insight into the ability of American ginseng to suppress colon cancer associated with colitis

Xiangli Cui[†], Yu Jin[†], Deepak Poudyal,
Alexander A.Chumanevich, Tia Davis¹,
Anthony Windust², Anne Hofseth, Wensong Wu³,
Joshua Habiger³, Edsel Pena³, Patricia Wood⁴,
Mitzi Nagarkatti⁵, Prakash S.Nagarkatti⁵ and
Lorne Hofseth*

Department of Pharmaceutical and Biomedical Sciences, South Carolina College of Pharmacy, University of South Carolina and Medical University of South Carolina, SC 29208, USA, ¹Department of Biological Sciences, University of South Carolina, Columbia, SC 29208, USA, ²Institute for National Measurement Standards, National Research Council, Ottawa, Canada, ³Department of Statistics, University of South Carolina, Columbia, SC 29208, USA, ⁴Wm. Jennings Bryan Dorn VA Medical Center and School of Medicine, University of South Carolina, Columbia, SC 29209, USA and ⁵Department of Pathology, Microbiology, and Immunology, School of Medicine, University of South Carolina, Columbia, SC 29209, USA

*To whom correspondence should be addressed. Department of Pharmaceutical and Biomedical Sciences South Carolina College of Pharmacy, 770 Sumter Street, Coker Life Sciences, Room 513C, University of South Carolina, Columbia, SC 29208, USA. Tel: +1 803 777 6627; Fax: +1 803 777 8356; Email: hofseth@cop.sc.edu

We have recently shown that American ginseng (AG) prevents and treats mouse colitis. Because both mice and humans with chronic colitis have a high colon cancer risk, we tested the hypothesis that AG can be used to prevent colitis-driven colon cancer. Using the azoxymethane (AOM)/dextran sulfate sodium (DSS) mouse model of ulcerative colitis, we show that AG can suppress colon cancer associated with colitis. To explore the molecular mechanisms of the anticancer effects of AG, we also carried out antibody array experiments on colon cells isolated at a precancerous stage. We found there were 82 protein end points that were either significantly higher (41 proteins) or significantly lower (41 proteins) in the AOM + DSS group compared with the AOM-alone (control) group. In contrast, there were only 19 protein end points that were either significantly higher (10 proteins) or significantly lower (9 proteins) in the AOM + DSS + AG group compared with the AOM-alone (control) group. Overall, these results suggest that AG keeps the colon environment in metabolic equilibrium when mice are treated with AOM + DSS and gives insight into the mechanisms by which AG protects from colon cancer associated with colitis.

Introduction

Numerous studies have established a link between colitis and colon cancer (1–3). The relative risk of colorectal cancer development in ulcerative colitis (UC) patients is 10-fold greater than in the general population (4) and this risk increases with duration of the colitis (2). The histopathogenesis of UC-associated colorectal cancer involves a stepwise progression from inflamed and hyperplastic epithelia, to flat dysplasia, to adenocarcinoma (5). Cancer appears to be derived through a multistep process, involving sequential alterations at the molecular and tissue levels. However, the specific molecular events have not been fully described, and little is known what occurs during

Abbreviations: AG, American ginseng; AOM, azoxymethane; CIS, carcinoma *in situ*; DSS, dextran sulfate sodium; H&E, hematoxylin and eosin; MAPK, mitogen-activated protein kinase; MEK1, mitogen activated protein kinase kinase 1; RSK, ribosomal S6 kinase; TNF, tumor necrosis factor; UC, ulcerative colitis.

[†]These authors contributed equally to this work.

colitis in mice. We have shown previously that American Ginseng (AG), a putative non-toxic antioxidant can both prevent and treat dextran sulfate sodium (DSS) and oxazolone-induced colitis in mice (6). As a continuation of these studies, here we describe an ability of AG to inhibit azoxymethane (AOM)/DSS-induced colitis-driven colon cancer. We also explore the mechanistic insight by demonstrating some molecular changes in precancerous colon epithelial cells from mice treated with AOM + DSS versus AOM/DSS + AG.

Materials and methods

American ginseng

The details and characteristics of AG have been described previously by our group in detail (6). An identical lot of AG has been used for these studies. Briefly, AG extract was purchased from the National Research Council of Canada. This extract was derived from roots of AG cultivated by Chai-Na-Ta Farms Ltd (Kamloops, British Columbia, Canada) and processed by Canadian Phytopharmaceuticals Corporation (Richmond, British Columbia, Canada). Following grinding to pass 80 mesh, 35 kg of the root material was extracted with aqueous ethanol (75% ethanol and 25% water) in a recirculating filter extraction system for 4 h at a temperature of 60°C under vacuum. The ratio of solvent to root was 8:1 (vol:wt). After extraction, the filtrate was partially dried *in vacuo* to yield a concentrated extract. Maltodextrin (2.8 kg) (40% of final weight) was then blended as a support and the resultant slurry was spray dried to yield 7 kg of free flowing powder. Analysis by Canadian Phytopharmaceuticals Corporation by high-performance liquid chromatography–ultraviolet against pure standards determined the total ginsenoside content (as the sum of: Rg1, Re, Rb1, Rc, Rb2 and Rd) of the finished material to be 10.1% (wt/wt) and confirmed by high-performance liquid chromatography–mass spectrometry at the National Research Council, Canada. The final, powder form of AG extract also contained 2% additional ginsenosides (made up of F11, Ro, isomers of Rd and traces of malonyl ginsenosides) and 40% of maltodextrin derived from hydrolyzed cornstarch. The remaining 48% of the powder was made up of ginseng root-derived polysaccharides/ligosaccharides and proteins and up to 5% of moisture. The lot utilized in this study was screened and found to comply with standards set (e.g. NSF/ANSI 173-03) for heavy metals and contaminants in dietary supplements and is periodically tested by National Research Council of Canada, Institute for National Measurement Standards to confirm stability of the ginsenoside content.

It should be noted here that regular AIN-93M chow fed to mice contains 12.5% maltodextrin. The addition of 75 p.p.m. AG in the chow equates to 30 mg/kg final concentration of maltodextrin added to 12.5% already in the chow. Therefore, there is 12.5% maltodextrin in the AIN-93M chow and 12.5003% of maltodextrin in the AIN-93M chow supplemented with 75 p.p.m. AG extract.

AOM/DSS-induced colon cancer model

We followed a modified protocol outlined recently by the Wirtz *et al.* (7). Supplementary Table 1 (available at *Carcinogenesis* Online) outlines the treatment groups for this model. Figure 1 outlines the time line. Briefly, 8- to 12-week-old male and female C57BL/6 mice were weighed and given a single intraperitoneal injection of AOM (10 mg/kg) or vehicle on experimental Day 1. One week later, animals received either 1% DSS in their drinking water or normal drinking water. At the same time, mice were given AIN 93M chow containing 0 or 75 p.p.m. AG. Chronic colitis was induced with cyclical DSS treatment, which consisted of 7 days of 1% DSS followed by 14 days of normal water for a total of three cycles. The AG was continued until the end of the experiment on Day 70. The AOM-only group was included to determine whether AG reduced colon cancer in the absence of inflammation. AG and DSS were initiated at the same time to test our initial hypothesis that AG can be used to prevent colon cancer associated with colitis and so that we could test carry out our protein array studies (described below) to compare the difference in epithelial cell protein changes between the AOM + DSS group and the AOM + DSS + AG group on Day 15.

To confirm that the AG was suppressing colitis, two mice from Groups 1, 3 and 7 were killed on Day 15 (see supplementary Table 1, available at *Carcinogenesis* Online, and Figure 1) and examined for acute inflammation by Swiss rolls, as we have described previously (6). A Swiss roll is a simple technique, where the entire colon can be removed, opened longitudinally and

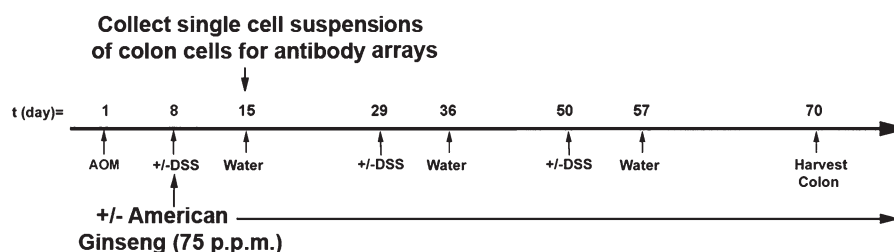


Fig. 1. Experimental protocol for the AOM/DSS mouse model of UC-driven colon cancer.

rolled with the mucosa outward. After histological processing, microscopical examination of the entire length of the colon is then possible. Five mice from the same groups were euthanized on the same day, and single-cell suspensions of epithelial/inflammatory cells were made and pooled from the five mice per group. To ensure no influence of age or sex on protein expression, all C57BL/6 mice used here were male and between 10 and 12 weeks of age. Colons were flushed out with phosphate-buffered saline, opened longitudinally and then incubated in 10% fetal calf serum/5 mM ethylenediaminetetraacetic acid/Ca/Mg-free phosphate-buffered saline for 15 min. Colons were then shaken gently for 10 s, and the single-cell suspension consisting of epithelial and inflammatory cells were collected in the supernatant. Trypan blue staining revealed >95% viable cells by microscopic observation. Epithelial cells were separated from inflammatory cells using magnetic cell sorting technology, according to kit instructions (mouse CD45 MicroBeads; Miltenyi Biotec, Auburn, CA). Pooled cell pellets from each group were frozen and sent to Kinexus Bioinformatics (Vancouver, Canada) for protein array analysis (see below). To our knowledge, there is no evidence for protein expression being affected by separating cells using antibody columns. Nevertheless, to reduce this possibility and any artifactual results, we processed all colons in all groups at the same time and in an identical manner at 4°C or on ice where applicable.

On Day 70, the remaining mice were weighed and euthanized, and their blood and tissues were harvested. Colons were cut longitudinally and fixed in 10% buffered formalin overnight. The colons were then stained with methylene blue and scored for the number of colonic macroscopic lesions, to determine the incidence (number of animals with at least one macroscopic lesion) and multiplicity (number of macroscopic lesions per animal) of macroscopic lesions. Macroscopic lesion area, based on length and width, was also calculated. Following photography, colons were rinsed with ice-cold phosphate-buffered saline and processed for histopathology [hematoxylin and eosin (H&E)] and immunohistochemistry by paraffin embedding.

Assessment of pathology

Following H&E staining, colons were assessed for tumor pathology in a blinded fashion by a trained pathologist. Low-grade dysplasias were defined as adenomatous changes, with simple glandular architecture, branching or elongation of crypts, a low nuclear to cytoplasmic ratio, cell nuclei elongated (picket fence look), nuclear crowding, stratified, hyperchromatic nuclei, changes extend to surface (not maturing), nuclei maintain polarity and nucleoli not conspicuous. High-grade dysplasias were defined as adenomatous changes with architectural complexities, a high nuclear to cytoplasmic ratio, increased mitosis, loss of normal gland architecture, variable gland size and shape, glands still have connective tissue core (space, collagen or cells) between them, tufting (back to back glands), loss of nuclear orientation, large cell nuclei (not basal), oval or round, pseudostratification, irregular nuclear membranes, large nucleoli and aberrant nuclei. Carcinoma *in situ* (CIS) was defined as a high-grade dysplasia plus nuclei big, piling up, bizarre bridging over/cribriform pattern (sieve-like), filling in of lumen with glands, loss of connective tissue core (no space or collagen or connective tissue or cells between glands, right next to each other) and glands within glands, back to back glands. The size of the abnormal pathology was defined as small (one villus involved) or large (>1 villus involved). All were adenomas, and there were no adenocarcinomas, consistent with some previous studies (8).

Antibody microarray

Protein from epithelial cells was isolated and scanned for protein expression using antibody microarrays (Kinexus Bioinformatics). Group 1 (AOM only) was the control group and compared with both the AOM + DSS group (Group 3) and AOM + DSS + AG group (Group 7). Analysis of protein extracts by such arrays was carried out in full by Kinexus Bioinformatics under a contractual agreement. The antibody microarray has the capability of quantitatively screening the expression of 800 individual proteins. The current full Kinex™ Service uses the KAM-1.2 chip with two samples analyzed in duplicate with 800 antibodies. The 500 pan-specific antibodies used in the chip provide for the

detection of 193 unique protein kinases, 24 protein phosphatases and 150 regulatory subunits of these enzymes and other cell signaling proteins that regulate cell proliferation, stress and apoptosis. This provides information about the expression levels of these target proteins. The 300 phospho-site-specific antibodies track the phosphorylation of 121 sites in protein kinases, 2 sites in protein phosphatases and 125 sites in other cell signaling proteins. In some cases, multiple antibodies from different commercial vendors have been used to monitor the expression or phosphorylation of the same target proteins.

Western blot analysis

Standard western blotting techniques were used. The antibodies used were: Phospho-c-Jun (Ser63) (Cat# 9261, 1:500; Cell Signaling Technology, Danvers, MA); Pax 2 (Cat# 2549-1, 1:500; Epitomics, Burlingame, CA); Phospho-Her2/ErbB2 (Tyr1248) (Cat# 2247, 1:500; Cell Signaling Technology); PP6C (Cat# 07-1224, 1:500; Millipore, Billerica, MA); EphA1 (Cat# sc-925, 1:500; Santa Cruz Biotechnology, Santa Cruz, CA) and IRAK1 (Cat# sc-5288; Santa Cruz Biotechnology).

Statistics

A chi-square contingency table analysis was done on the AOM/DSS and AOM/DSS plus AG inhibitor groups to determine if there is a statistically significant difference in their inflammation scores. Macroscopic lesion incidence was examined using a Fisher's exact test, which is equivalent to a test for binomial proportions. Because the usual assumptions underlying the analysis of variance test are not satisfied in assessing the significance of the *F*-statistic value from the analysis of variance table, instead of using the *F*-distribution, we used a permutation distribution to examine macroscopic lesion multiplicity. A non-parametric Kruskal–Wallis test was used to compare mean macroscopic lesion area. A Fisher's exact test was used to test the significance of association between treatments and classifications (low grade, high grade and CIS). Protein expression levels were assumed to either follow a zero-mean normal distribution (null case) if the protein is non-differentially expressed or three types of mixtures of normals (alternative) if differentially expressed. Using maximum likelihood estimation via the expectation–maximization algorithm and Akaike's An Information Criterion, the posterior probabilities that proteins follow the mixture normal distribution were computed, and those with probabilities of at least 95% were declared differentially expressed. The *P*-value chosen for significance in this study was 0.05.

Results

AG suppresses AOM + DSS-induced macroscopic lesions

We have shown previously that AG suppresses colitis (6). Because both mice and humans with chronic colitis are at a high risk for colon cancer, here, we tested the hypothesis that AG prevents the onset of colon cancer in a mouse model of colitis-driven colon cancer. Following 70 days (Figure 1), colons were harvested and stained with methyl blue to examine macroscopic lesions. Table I shows that the 88% of mice treated with AOM + DSS, but 0% in all other groups (AOM, DSS, AG, AOM + AG and DSS + AG) had macroscopic lesions. A total of 20% (2/10) mice treated with AOM + DSS + AG (75 p.p.m.) had macroscopic lesions. This difference was statistically significant using a Fisher's exact test ($P < 0.05$).

Macroscopic lesion multiplicity (number of macroscopic lesions per animal) also decreased with AG treatment (Table I). The total number of macroscopic lesions in the AOM + DSS group was 70 and the total number of macroscopic lesions in the AOM + DSS + AG group was 5. Permutation distribution analysis found similar results to that of incidence. The difference between the AOM + DSS

(4.6 ± 0.9 macroscopic lesions per animal) and AOM + DSS + 75 p.p.m. AG (0.5 ± 0.41 macroscopic lesions per animal) was statistically significant ($P < 0.05$). Finally, macroscopic lesion area (square millimeter) also decreased with AG treatment (Table I). The mean area of macroscopic lesions in the AOM + DSS group was 2.8 ± 0.3 mm² and the mean area of macroscopic lesions in the AOM + DSS + AG group was 0.8 ± 0.3 mm² ($P < 0.05$). Figure 2A shows typical colons from each group after staining (arrows point to a macroscopic lesion); Figure 2B shows representative H&E sections of the indicated group.

AG suppresses the severity of microscopic colon adenomas associated with AOM + DSS

Because many lesions are not macroscopically evident, as well as some growths are not necessarily cancerous under a microscope, we

Table I. Macroscopic lesion incidence and multiplicity in mice treated with AOM/DSS ± AG

Group	N	% Animals with macroscopic lesions (incidence)	Number of macroscopic lesions per animal (multiplicity) mean ± SE	Average area of macroscopic lesions (mm ²) mean ± SE
AOM	10	0	0	—
DSS	7	0	0	—
AOM + DSS	16	88	4.6 ± 0.9	2.8 ± 0.3
AG	4	0	0	—
AOM + AG	10	0	0	—
DSS + AG	6	0	0	—
AOM + DSS + AG	10	20 ^a	0.5 ± 0.4 ^a	0.8 ± 0.3 ^a

^aIndicates significant difference from AOM + DSS-treated group (see Materials and Methods for Statistics).

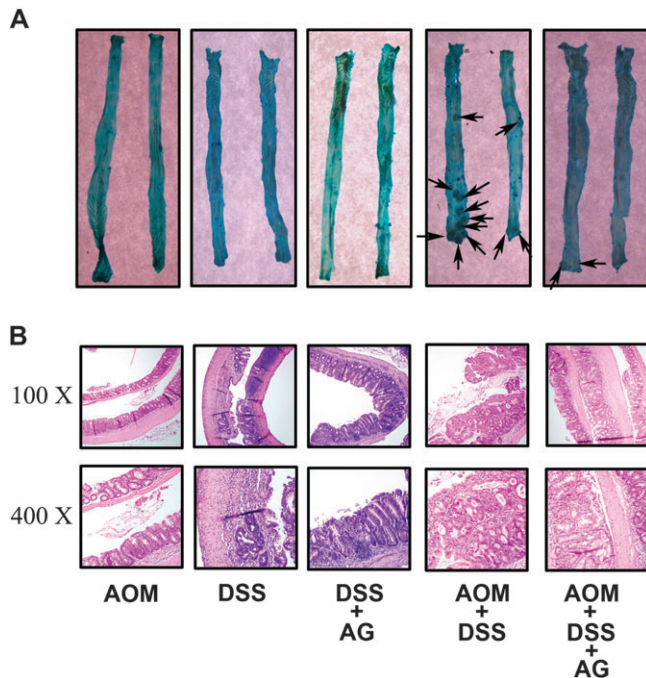


Fig. 2. Tumor formation in colons of mice treated with AOM + DSS is prevented when these mice consume AG (75 p.p.m.) in their chow. (A) Colons stained with methylene blue. Arrows indicate macroscopic tumors. (B) Representative H&E sections. The DSS-only group shows an area of ulceration and inflammation. The AOM + DSS group shows a polypoid adenoma with high-grade dysplasia, characteristic of tumors in this group.

next sectioned each colon and examined by histology. As shown in Table II, the addition of AG to the diet of AOM + DSS-treated mice dramatically lowered the severity of microscopically observed adenomas present. Only 25.5% of total microscopic lesions were classified as low-grade dysplasia in the AOM + DSS group. In contrast, almost 3-fold (62.5%) of total microscopic lesions were in the same category when AG was added to the chow. This trend shifted when looking at microscopic lesions of high grade and/or CIS. Lesions (74.5%) were of high grade and/or CIS in the AOM + DSS group, whereas only one half (37.5%) of the lesions were in the same high-grade/CIS category when AG was added to the chow. Using Fisher's exact test, the association between treatments (AOM + DSS versus AOM + DSS + AG) and classifications (low grade versus high grade versus CIS) was significant ($P = 0.02$), indicating a strong association. As indicated, no lesions were classified as adenocarcinomas, consistent with other similar studies (8,9).

Effects of AG on the expression of inflammation and cancer markers: screening of 800 biomarkers

To better understand the mechanisms of actions of AG at a precancerous level, we collected single-cell suspensions of colon epithelial cells (separated from other cells such as inflammatory cells) and screened for 800 biomarkers using an antibody microarray. To do this, we collected colon tissues after AOM injection and one cycle of DSS (see Figure 1 and supplementary Table 1 is available at *Carcinogenesis* Online). As mentioned in the Materials and Methods, to reduce the possibility of artifactual results, we processed all colons in all groups at the same time and in an identical manner at 4°C or on ice where applicable. We first confirmed that inflammation was higher in the AOM + DSS versus the AOM-only group and lower in the AOM + DSS + AG group versus the AOM + DSS group by measuring colon length. As we have shown previously, colon length shrinks when inflamed (6,10). Results indeed showed that colon length was 7.6 ± 0.09 cm in the AOM group, 6.6 ± 0.29 cm in the AOM + DSS group and 8.3 ± 0.1 cm in the AOM + DSS + AG group. Results were confirmed by histopathological evaluation of inflammatory index of colons on two separate mice from each group (data not shown). Separate mice had to be used for such purposes because inflammatory index was gauged by H&E staining. At the same time, we processed colon epithelial cells from five separate mice for examination by the Kinexus antibody microarray [Kinex™ Antibody Microarray (KAMS-1.2)].

We first compared the AOM to the AOM + DSS group. The proteins whose posterior probability of being differentially expressed (that is at least 0.95) are shown in supplementary Table 2, available at *Carcinogenesis* Online. In brief, there were 82 protein end points that were either significantly higher (41 proteins) or significantly lower (41 proteins) in the AOM + DSS group compared with the AOM-alone (control) group. In contrast, there were only 19 protein

Table II. Histological tumor incidence and multiplicity in mice treated with AOM/DSS ± AG

Group	N	% of microscopic lesions classified as low-grade dysplasia		% of microscopic lesions classified as high-grade dysplasia		% of microscopic lesions classified as CIS
		Small	Large	Small	Large	
AOM	10	0	0	0	0	0
DSS	7	0	0	0	0	0
AOM+DSS	10	7	18.5	3.7	44.4	26.4
AG	4	0	0	0	0	0
AOM + AG	10	0	0	0	0	0
DSS + AG	6	0	0	0	0	0
AOM + DSS + AG	10	43.7	18.8	12.5	12.5	12.5

end points that were either significantly higher (10 proteins) or significantly lower (9 proteins) in the AOM + DSS + AG group compared with the AOM-alone (control) group (supplementary Table 3 is available at *Carcinogenesis* Online).

It stands to reason that proteins upregulated to a similar extent in both supplementary Tables 2 and 3 (available at *Carcinogenesis* Online) are unlikely candidates targets for the protective effects of AG in the AOM + DSS model. Such proteins include DNAPK (DNA-activated protein-serine kinase), p38 MAPK (mitogen activated protein-serine kinase p38 alpha), Erk4 (extracellular signal-regulated kinase 4) and Phospho T-538 PKC ζ (protein-serine kinase C theta). However, COT [Osaka thyroid oncogene protein-serine kinase (Tpl2)] and Erk1 [extracellular signal-regulated kinase 1 (p44 MAPK)] were both 4-fold upregulated in the AOM + DSS + AG group than in the AOM + DSS group when compared with the AOM control.

Similarly, proteins downregulated to a similar extent in both supplementary Tables 2 and 3 (available at *Carcinogenesis* Online) are also unlikely candidates for the protective effects of AG in the AOM + DSS model. These include FLT4 [vascular endothelial growth factor receptor-protein-tyrosine kinase 3 (VEGFR3)], phosphor-Y577 FAK (focal adhesion protein-tyrosine kinase), phospho-S657 PKC α (protein-serine kinase C alpha), RSK1 (ribosomal S6 protein-serine kinase 1), PKB β (Akt2) (protein-serine kinase B beta) and phosphor-Y84 BLNK (B-cell linker protein).

TTK (dual specificity protein kinase) was downregulated in both groups, but significance was only reached in the AOM + DSS + AG group. Expression of CDK1 (cyclin-dependent protein-serine kinase 1) and phospho-T394 MEK2 [mitogen-activated protein kinase (MAPK)/ERK protein-serine kinase 2] were both elevated in the AOM + DSS group but significantly downregulated in the AOM + DSS + AG group. Although DAXX (death-associated protein 6) and LcK (lymphocyte-specific protein-tyrosine kinase) were increased slightly in the AOM + DSS group, significance was only reached in the AOM + DSS + AG group.

Table III lists the candidate molecules that are potentially responsible for AOM + DSS-induced cancer and suppression of these cancers by the addition of AG to the diet. Table IIIA shows proteins that are elevated significantly in the AOM + DSS group (therefore indicating possible tumor promoter properties) but not in the AOM + DSS + AG group. These include phospho-S63 Jun, phospho-S394 Pax2 (paired box protein 2), phospho-Y1248 ErbB2 (HER2), PARP1 [poly (adenosine diphosphate-ribose) polymerase 1], phospho-S910 PKC μ (PKD) (protein-serine kinase C mu/protein kinase D), phospho-T410/T403 PKC ζ /1 (protein-serine kinase C zeta/lambda), Erk5 (extracellular signal-regulated kinase 5), PKA R2a (cyclic adenosine 3',5'-monophosphate-dependent protein-serine kinase regulatory type 2 subunit alpha), Hsp90 (heat shock protein 90 kDa protein alpha/beta), SODD (silencer of death domains), ErbB2 (HER2) (ErbB2 (Neu) receptor-tyrosine kinase) and phospho-T693 EGFR (epidermal growth factor receptor-tyrosine kinase).

To confirm the results from the antibody array, we examined lysates by western blot. In addition to epithelial cell lysates (CD45 $-$ cells), we also probed lysates from inflammatory (CD45 $+$) cells. Figure 3 shows that the three proteins/modifications listed on the top of Table IIIB (phospho-S63 Jun, phospho-S394, Pax2 and phospho-Y1248 ErbB2) were indeed elevated in the epithelial lysates (CD45 $-$ cells) from the AOM + DSS mice and AG suppressed this elevation.

In contrast, there are proteins that are all significantly downregulated in the AOM + DSS group but not downregulated or expression is increased in the AOM + DSS + AG group (Table IIIA). These data indicate such end points are potential tumor suppressors, where expression is reduced by AOM + DSS and that this decreased expression is protected by the addition of AG. Such proteins include phospho-T385 mitogen activated protein kinase kinase 1 (Mek1) (MAPK/ERK protein-serine kinase 1), IR/IGF1R (insulin receptor/insulin-like growth factor 1 receptor), IRAK1 (interleukin 1 receptor-associated kinase 1), Crystallin (crystallin alpha B), PP6C (protein-serine phosphatase 6 catalytic subunit), CDC2L5 (cell division cycle 2-like protein-serine kinase 5), Hsp60 (heat shock protein 60 kDa protein 1),

CaMK1 γ (calcium/calmodulin-dependent protein-serine kinase 1 gamma), phospho-S363/S369 RSK1/2 (phospho-serine363/serine369-ribosomal S6 protein-serine kinase), CaMK2 α (calcium/calmodulin-dependent protein-serine kinase 2 alpha) and PP1/Ca (protein-serine phosphatase 1—catalytic subunit—alpha isoform).

Again, to confirm results from the antibody array, we examined lysates by western blot. In addition to epithelial cell lysates (CD45 $-$ cells), we again probed lysates from inflammatory (CD45 $+$) cells. Figure 3 shows that the three proteins/modifications listed on the top of Table IIIA (PP6C, EphA1 and IRAK1) were indeed reduced in the epithelial lysates (CD45 $-$ cells) from the AOM + DSS mice and AG offset this reduction.

Discussion

There is increasing attention being paid to complementary and alternative strategies for the prevention of high cancer risk, radical species overload diseases (11). This is mostly because of serious side effects associated with conventional treatment strategies of such diseases at a precancerous stage. Since we have recently shown that AG can be used to prevent and treat mouse colitis (6), we tested the hypothesis that AG can prevent colon cancer associated with colitis. Using the AOM/DSS mouse model of UC, we show here for the first time that results are consistent with this hypothesis.

Many studies have shown anticancer effects of AG *in vitro*. For example, ginseng and ginseng components can induce apoptotic genes and suppress cell-cycle mediators (12,13) and enhance the anticancer effects of standard chemotherapeutic agents (14) in colon cancer cell lines. Increasingly, *in vivo* models have shown an anticancer effect of ginseng components. One of the earliest studies done to show a chemopreventive effect of ginseng appeared in the literature >25 years ago. Yun *et al.* (15) found that the prolonged administration of Korean red ginseng extract inhibited the incidence as well as the proliferation of tumors induced by 7,12-dimethylbenz(a)anthracene, urethane and aflatoxin B1. More recently, ginseng components have been shown to inhibit metastases (16,17), as well as inhibit the growth of tumor xenografts (18) in animals. Some forms of ginseng have been shown to inhibit angiogenesis (19), inhibit benzo[a]pyrene-induced lung tumorigenesis in mice (20), inhibit hepatocarcinogenesis in mice (21) as well as show promise in improving quality of life and reducing mortality from human cancers (22). Ginseng can also enhance the effects of standard therapeutic regimens against cancer (23,24).

With respect to colon cancer, others have shown that ginseng can inhibit the formation of aberrant crypt foci in rat colon cancer models (25). Ginseng has also been shown to inhibit the expression of inflammatory markers in *Helicobacter pylori*-infected cells (26). As well, we and others have shown an ability of ginseng to inhibit the activation of inflammatory cells and therefore inhibit resultant pro-carcinogenic epithelial damage (6,27).

The molecular mechanisms of the anticancer effects of ginseng *in vivo* are not completely understood. To bridge this understanding, we carried out antibody array analysis of protein collected from colon epithelial cells at a precancerous stage (Figure 1) but exposed to chronic inflammation. To our knowledge, we provide the first set of data screening putative candidate proteins/protein subunits/protein modifications responsible for or associated with the onset of adenomas associated with AOM + DSS treatment. Additionally, we provide insight into candidate proteins responsible for the protective effects of AG in AOM + DSS-treated mice (Table III and Figure 3).

Proteins/protein subunits/protein modifications shown to be upregulated in the AOM + DSS group but not changed or downregulated by AG represent possible targets of AOM + DSS to drive inflammation-associated colon cancer. We have identified 11 such candidate tumor oncogenes/tumor promoters in this particular model of colon cancer (Table III).

Jun is a well-documented proto-oncogene in many cancers including colon cancer (28). Among many mechanisms, this transcription factor cooperates with oncogenic alleles of ras in malignant transformation. Constitutively active Ras causes (via activation of MAPKs)

Table III. Target proteins identified as potentially key to the protective effects of AG on AOM + DSS-induced tumorigenesis

Protein end point	Fold change		Site of antibody binding	Full protein name
	AOM+DSS/AOM	AOM+DSS+AG/AOM		
(A) Proteins with lower expression in AOM + DSS group but not lower or elevated in the AOM + DSS + AG group versus AOM-alone group (indicating possible tumor suppressor properties that are protected by AG)				
PP6C	0.28*	8.93*	Pan-specific	Protein-serine phosphatase 6—catalytic subunit (PPVC)
EphA1	0.81	5.85*	Pan-specific	Ephrin type-A receptor 1 protein-tyrosine kinase
IRAK1	0.19*	2.10	Pan-specific	Interleukin 1 receptor-associated kinase 1 (Pelle-like protein kinase)
Mek1	0.18*	1.06	T385	Phospho-T385-MAPK/ERK protein-serine kinase 1 (MKK1)
IR/IGF1R(INSR)	0.17*	1.70	Y1189/Y1190	Phospho-Y1189/Y1190-Insulin receptor / Insulin-like growth factor 1 receptor
Crystallin	0.22*	1.07	Pan-specific	Crystallin alpha B (heat-shock 20 kDa like-protein)
CDC2L5	0.30*	1.08	Pan-specific	Cell division cycle 2-like protein-serine kinase 5
CaMK1g	0.31*	2.43	Pan-specific	Calcium/calmodulin-dependent protein-serine kinase 1 gamma
RSK1/2	0.31*	1.32	S363/S369	Phospho-S363/S369-Ribosomal S6 protein-serine kinase 1/2
CaMK2a	0.31*	1.23	T286	Phospho-T286-Calcium/calmodulin-dependent protein-serine kinase 1 gamma
PP1/Ca	0.32*	1.07	Pan-specific	Protein-serine phosphatase 1—catalytic subunit—alpha isoform
(B) Proteins with elevated expression in AOM + DSS group but not elevated or lowered in the AOM + DSS + AG group versus AOM-alone group (indicating possible tumor promoting properties that are inhibited by AG)				
Jun	27.85*	0.85	S63	Phospho-S63-Jun
Pax2	9.14*	0.66	S394	Phospho-S394-Paired box protein 2
ErbB2 (HER2)	5.64*	0.80	Y1248	Phospho-Y1248-ErbB2 (Neu) receptor-tyrosine kinase
PARP1	5.42*	0.88	Pan-specific	Poly [ADP-ribose] polymerase 1 (ADPRT)
PKCm	4.96*	0.42	S910	Phospho-S910-Protein-serine kinase C mu (Protein kinase D)
PKCz/l	4.29*	0.75	T410/T403	Phospho-T410/T402-Protein-serine kinase C zeta/lambda
Erk5	4.25*	0.88	Pan-specific	Extracellular signal-regulated kinase 5 [Big MAP kinase 1 (BMK1)]
PKA R2a	4.17*	0.95	Pan-specific	cAMP-dependent protein-serine kinase regulatory type 2 subunit alpha
Hsp90	4.16*	0.29	Pan-specific	Heat shock 90 kDa protein alpha/beta
SODD	4.10*	0.82	Pan-specific	Silencer of death domains [Bcl2 associated athanogene 4 (BAG4)]
ErbB2 (HER2)	3.74*	0.73	Pan-specific	ErbB2 (Neu) receptor-tyrosine kinase
EGFR	3.35*	0.83	T693	Phospho-T693-epidermal growth factor receptor-tyrosine kinase

Asterisks indicate significantly differential expression compared with the AOM-only group.

IRAK1, interleukin 1 receptor-associated kinase 1; MEK1, mitogen activated protein kinase kinase 1; MAPK, mitogen-activated protein kinase; cAMP, cyclic adenosine 3',5'-monophosphate.

phosphorylation of c-Jun, which is essential for subsequent target gene activation and tumorigenesis (29). We should note here, that we found the phosphorylated form of Jun to be upregulated. c-Jun has also been shown to antagonize the activity of the potent tumor suppressor protein, p53 (30).

The PAX gene encodes DNA-binding proteins and plays a role in embryogenesis and carcinogenesis [31]. Upregulation of PAX2 is observed in prostate cancer, ovarian carcinomas, renal cancer and colon

cancer and is used as a diagnostic marker in primary renal tumors (32). Apoptosis is induced in cancer cells by the inhibition of PAX2, possibly because PAX2 acts as a transcriptional repressor of p53 (33).

ErbB2 (her2) is an oncogenic protein that belongs to the ErbB family of receptor tyrosine kinases and is implicated in tumor progression. It is often overexpressed in epithelial tumors, including colon cancer (34). Most notably, ErbB2 has been a key target in the treatment of breast cancers, where approximately 15–20% of breast

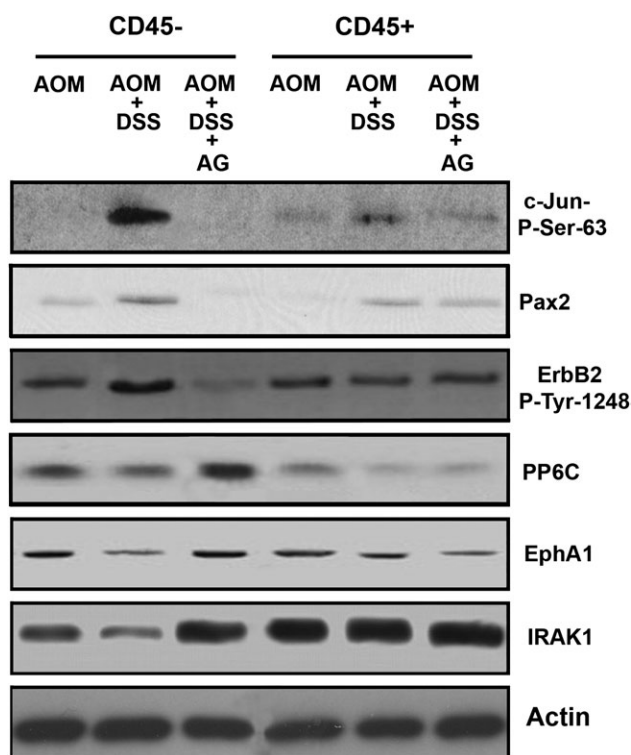


Fig. 3. Confirmation of antibody array data by western blot analysis. Lysates from CD45⁻ epithelial cells and CD45⁺ inflammatory cells were examined in AOM, AOM + DSS and AOM + DSS + AG groups. Results shown for the CD45⁻ epithelial cells are consistent with antibody array data analysis for six of the proteins/posttranslational modifications.

cancers have an amplification of this gene or overexpression of its protein product (35). Interestingly, ErbB2 and EGFR [which is overexpressed in cervical, breast, prostate and colon cancers (36–38)] are key mediators of tumor necrosis factor (TNF)-regulated anti-apoptotic signals in intestinal epithelial cells. Specifically, loss of ErbB2 or EGFR expression increases TNF-induced apoptosis (39). Given evidence for TNF signaling in the development of colitis-associated carcinoma, this observation has significant implications for understanding the role of EGFR in maintaining intestinal epithelial cell homeostasis during cytokine-mediated inflammatory responses.

Extracellular signal-regulated kinase 5 (Erk5) is a member of the MAPK family. Erk5 is a tumor promoter and is reported to inhibit apoptosis of endothelial cells *in vitro* (40). Inhibition of Erk5 expression by microRNA-143 contributes to Jurkat cell apoptosis and colon cancer DLD-1 cell growth suppression (41). Interestingly, Erk5 plays an essential role in the upregulation of cyclooxygenase-2 in colon cancer cells (42). Similarly, it has been shown that PKCmu (PKD) plays a key role in the upregulation of Cox-2 by pro-inflammatory cytokines in colonic subepithelial myofibroblasts (43). In CD95-sensitive Colo357 cells, forced overexpression of PKCmu strongly reduced CD95-mediated apoptosis. In addition, PKCmu overexpression led to a strongly enhanced cell growth and to a significant increase of telomerase activity (44). PKCzeta and lambda levels were also elevated in AOM + DSS-treated groups and suppressed by the addition of AG. The upregulation of particulate PKCzeta has been implicated in rat colonic carcinogenesis (45,46), consistent with our findings.

SODD is a widely expressed anti-apoptotic protein. It binds to the TNF- α receptor and prevents spontaneous self-association of death domains and inappropriate receptor signaling. In addition, overexpression of SODD suppresses TNF- α -induced cell death (47). Interestingly, mice lacking SODD produce larger amounts of cytokines in

response to *in vivo* TNF challenge. In addition, TNF-induced activation of nuclear factor-kappaB is accelerated in SODD-deficient cells, consistent with the understanding that SODD is critical for the regulation of TNF signaling (48).

PKA R2a is highly expressed in a somatomammotroph GH3 cell line and in pituitary adenomas, whereas less expressed in cortisol-secreting adrenocortical tumors (49,50). The role of PKA is dependent on its location and balanced expression between regulatory subunit 1 (R1) and regulator subunit 2 (R2). The R2-selective cyclic adenosine 3',5'-monophosphate analog 8-Cl cyclic adenosine 3',5'-monophosphate and R1A RNA silencing stimulates cell proliferation and increases Cyclin D1 expression, respectively, in human and rat adenomatous somatotrophs. These data indicate that a low R1:R2 ratio promotes proliferation (49). PKA inhibition in pancreatic cancer cells has been shown to lead to growth arrest and apoptosis (51). The role of PKA R2a in colon carcinogenesis, however, remains unclear.

HSP 90 inactivates *v-src* oncogene product transformation when complexed with *src* (52). Inhibition of HSP90 activity is the key to the degradation of oncoproteins such as Erb B2 and thus is considered an anti-neoplastic target in diverse human tumors including colon (52–54). HSP 90 inhibitors have been developed as anti-cancer drugs in preclinical trials (55,56). It is very important to the stability and function of multiple cancer-related proteins, such as ERB-B2 (EGFR) and VEGFR and is crucial to cancer cell growth and survival (53).

PARP1 is a stability protein that is found expressed in neoplastic tissues. It is a nuclear enzyme that signals the presence of DNA damage by catalyzing the addition of adenosine diphosphate-ribose units to DNA, histones and various DNA repair enzymes and by facilitating DNA repair. Inhibition of PARP potentiates the activity of DNA-damaging agents, including chemotherapeutics and radiation. PARP1 is reported to play role in early stage of colorectal carcinogenesis (57) and possibly in metastases in mouse colon carcinoma cells (58). There are currently a number of clinical trials testing the ability of PARP inhibitors as a cancer treatment strategy (59).

Proteins shown to be downregulated in the AOM + DSS group but not changed or upregulated by AG represent putative tumor suppressors in the AOM + DSS model. We have identified 11 such candidate tumor suppressors in this particular model of colon cancer. Interleukin 1 receptor-associated kinase (IRAK1s) are key mediators in the signaling pathways of toll-like receptors/interleukin-1 receptors (IL-1Rs). IRAK1 can initiate a cascade of signaling events eventually leading to induction of inflammatory target gene expression (60). Given this, it was interesting to find that this molecule is downregulated in the AOM + DSS epithelial cells. Because this finding was confirmed by western analysis, we are unable to explain the result at this time. It is possible that although IRAK1 levels are unchanged in the inflammatory cell lysates and downregulated in the epithelial cells from AOM + DSS mice, IRAK1 activity is elevated. We are currently exploring this hypothesis.

Interestingly, two proteins (PPI/Ca and PP6C) belonging to protein kinases family are found to be putative tumor suppressors in our studies. This result is consistent with other studies. PPI inhibitors have been found to be pro-carcinogenic (61). Little is known about the role of PP6/Ca in carcinogenesis. It does play a role in a DNA damage response because silencing of PP6c by small interfering RNA induces sensitivity to irradiation and delayed release from the G₂/M checkpoint (62).

Inconsistent with previous studies, we have found that there are several tumor-promoting proteins to be suppressed by AOM + DSS but not when AG was added to the diet. For example, MAPK kinase MEK1 is known to promote carcinogenesis. Recently it has been found that constitutive activation of MEK1 in intestinal epithelial cells is sufficient to induce an epithelial-to-mesenchymal transition associated with colon tumor invasion and metastasis (63). Potent and selective inhibitors of MEK1 and MEK2 have been developed as well and are currently in phase I/II clinical trials (64). Insulin-like growth

factor-I (IGF-I), IGF-II and insulin have recently been found to be involved in regulating several different signaling pathways related to carcinogenesis via the type I IGF receptor (IGF1R) and insulin receptor (IR). Upregulated IGF1R/IR has been shown in cell culture, animal studies and human diseases to be involved in malignant transformation, progression and metastasis (65,66).

Since the differential expression during tumorigenesis and metastasis in various epithelial tumors, Alpha-B-crystallin, a small heat-shock protein, has recently been shown to be involved in cancer biology. It is described as a molecular regulator of cyclin-D1 ubiquitination and inhibits pro-apoptotic proteins such as caspase-3, p53, Bax and Bclx's and TNF-related apoptosis-inducing ligand resistance in numerous human cancer cell lines (67–70)). Consistent with our findings, however, is that alpha-B-crystallin expression is high in normal colon tissues (71), but absent in colon cancer tissue (72).

There is little known about the physiological functions of CDC2L5, which is also downregulated by AOM + DSS treatment. It has been shown that it is a Cdk-like kinase, and there is a functional role of the CDC2L5 kinase in splicing regulation (73). The Ca²⁺/calmodulin-dependent protein kinases (CaMKs) are multifunctional serine/threonine kinases whose activity is regulated through Ca²⁺ signaling (74). The most widely studied CaMKs include CaMKI and CaMKII. The CaMKs regulate the development and activity of multiple different cell types. CaMKI and II expression has been found in endometrial cancer cells and correlates with malignant potential of this tumor (75). The specific role of CAMK1g in tumorigenesis is also unclear, however.

Although its biological functions are not well elucidated, ribosomal S6 kinase (RSK) is an important downstream effector of MAPK. From clinical pathological investigation of tumor samples, overexpressed RSK has been found in ~50% of human breast cancer tissues (76). Targeted inhibition of RSK can also phosphorylate and inactivate Bad via a PKC-dependent and Erk-independent pathway in gastric cancer cells (77). These findings suggest that RSK plays a role in proliferation of transformed cells and may be a new prospective drug target for chemotherapeutic agents.

Overall, we have shown that AG suppresses tumorigenesis in the AOM + DSS mouse model of colitis. Importantly, we provide some mechanistic insight into these findings. More specifically, by isolating colon epithelial cells at a relatively early stage of the process, where cells have yet to be identified pathologically as cancerous, we have parsed out 11 proteins that were upregulated in AOM + DSS-treated mice, but not in AOM + DSS + AG-treated mice. All have putative or known tumor promoting properties, suggesting that AOM + DSS promote colon tumorigenesis through the activation of one or more of these molecules, and AG suppresses this activation. Of the 11 proteins we identified as being suppressed by AOM + DSS, few have putative or known tumor suppressor properties. Surprisingly, many have tumor-promoting properties. There are several possibilities for this latter finding, including the particular model we have used here, and a differential role for these particular proteins in our model. Another possibility is that these particular proteins do not play a role in tumorigenesis in the AOM + DSS mouse model. Together, though, we provide several possible candidate proteins involved in AOM + DSS-induced colon carcinogenesis and that one or more of these candidates are a target by which AG protects from AOM + DSS-induced colon carcinogenesis. The general finding that 82 protein end points were significantly changed in the AOM + DSS group compared with the AOM-alone (control) group, but only 19 protein endpoints were significantly changed in the AOM + DSS + AG group is consistent with the hypothesis that AG keeps the colon environment in metabolic equilibrium when mice are treated with DSS.

Supplementary material

Supplementary Tables 1–3 can be found at <http://carcin.oxfordjournals.org/>

Funding

Center for CAM Research on Autoimmune and Inflammatory Diseases, National Institutes of Health (1P01AT003961-01A1 to P.S.N., L.J.H. and M.N.); COBRE funded University of South Carolina Center for Colon Cancer Research, National Institutes of Health (P20RR17698-01) (Franklin Berger, Director); Immunotoxicology Core (1P01AT003961-01A1, Dr Narendra Singh, Director), Mouse Core (P20RR17698-01, Dr Marj Pena, Director); Imaging/Histology Core (P20RR17698-01).

Acknowledgements

We thank Immunotoxicology Core (Dr Narendra Singh, Director), Mouse Core (Dr Marj Pena, Director) and Imaging/Histology Core.

Conflict of Interest Statement: None declared.

References

- Lennard-Jones, J.E. *et al.* (1983) Cancer surveillance in ulcerative colitis. Experience over 15 years. *Lancet*, **2**, 149–152.
- Lashner, B.A. *et al.* (1990) Colon cancer surveillance in chronic ulcerative colitis: historical cohort study. *Am. J. Gastroenterol.*, **85**, 1083–1087.
- Kiesslich, R. *et al.* (2003) Methylene blue-aided chromoendoscopy for the detection of intraepithelial neoplasia and colon cancer in ulcerative colitis. *Gastroenterology*, **124**, 880–888.
- Askling, J. *et al.* (2001) Family history as a risk factor for colorectal cancer in inflammatory bowel disease. *Gastroenterology*, **120**, 1356–1362.
- Rubin, D.T. *et al.* (2008) Colorectal cancer prevention in inflammatory bowel disease and the role of 5-aminosalicylic acid: a clinical review and update. *Inflamm. Bowel Dis.*, **14**, 265–274.
- Jin, Y. *et al.* (2008) American ginseng suppresses inflammation and DNA damage associated with mouse colitis. *Carcinogenesis*, **29**, 2351–2359.
- Wirtz, S. *et al.* (2007) Chemically induced mouse models of intestinal inflammation. *Nat. Protoc.*, **2**, 541–546.
- Onizawa, M. *et al.* (2009) Signaling pathway via TNF- α /NF- κ B in intestinal epithelial cells may be directly involved in colitis-associated carcinogenesis. *Am. J. Physiol. Gastrointest. Liver Physiol.*, **296**, G850–G859.
- Clapper, M.L. *et al.* (2008) 5-aminosalicylic acid inhibits colitis-associated colorectal dysplasias in the mouse model of azoxymethane/dextran sulfate sodium-induced colitis. *Inflamm. Bowel Dis.*, **14**, 1341–1347.
- Kotakadi, V.S. *et al.* (2008) Ginkgo biloba extract EGB 761 has anti-inflammatory properties and ameliorates colitis in mice by driving effector T cell apoptosis. *Carcinogenesis*, **29**, 1799–1806.
- Hofseth, L.J. *et al.* (2007) Inflammation, cancer, and targets of ginseng. *J. Nutr.*, **137**, 183S–185S.
- Wang, C.Z. *et al.* (2009) Antiproliferative effects of different plant parts of Panax notoginseng on SW480 human colorectal cancer cells. *Phytother. Res.*, **23**, 6–13.
- Luo, X. *et al.* (2008) Characterization of gene expression regulated by American ginseng and ginsenoside Rg3 in human colorectal cancer cells. *Int. J. Oncol.*, **32**, 975–983.
- Li, X.L. *et al.* (2009) Panaxadiol, a purified ginseng component, enhances the anti-cancer effects of 5-fluorouracil in human colorectal cancer cells. *Cancer Chemother. Pharmacol.*, **11**, 11.
- Yun, T.K. *et al.* (1983) Anticarcinogenic effect of long-term oral administration of red ginseng on newborn mice exposed to various chemical carcinogens. *Cancer Detect. Prev.*, **6**, 515–525.
- Xu, T.M. *et al.* (2008) Inhibitory effect of ginsenoside Rg3 on ovarian cancer metastasis. *Chin. Med. J. (Engl.)*, **121**, 1394–1397.
- Park, T.Y. *et al.* (2008) Anti-metastatic potential of ginsenoside Rp1, a novel ginsenoside derivative. *Biol. Pharm. Bull.*, **31**, 1802–1805.
- Wang, W. *et al.* (2008) Experimental therapy of prostate cancer with novel natural product anti-cancer ginsenosides. *Prostate*, **68**, 809–819.
- Carneiro, C.S. *et al.* (2007) Pfaffia paniculata (Brazilian ginseng) methanolic extract reduces angiogenesis in mice. *Exp. Toxicol. Pathol.*, **58**, 427–431.
- Yan, Y. *et al.* (2006) Efficacy of polyphenon E, red ginseng, and rapamycin on benzo(a)pyrene-induced lung tumorigenesis in A/J mice. *Neoplasia*, **8**, 52–58.
- da Silva, T.C. *et al.* (2005) Inhibitory effects of Pfaffia paniculata (Brazilian ginseng) on preneoplastic and neoplastic lesions in a mouse hepatocarcinogenesis model. *Cancer Lett.*, **226**, 107–113.

22. Cui, Y. *et al.* (2006) Association of ginseng use with survival and quality of life among breast cancer patients. *Am. J. Epidemiol.*, **163**, 645–653.
23. Chen, F.D. *et al.* (2001) Sensitization of a tumor, but not normal tissue, to the cytotoxic effect of ionizing radiation using Panax notoginseng extract. *Am. J. Chin. Med.*, **29**, 517–524.
24. Lee, S.J. *et al.* (1999) Antitumor activity of a novel ginseng saponin metabolite in human pulmonary adenocarcinoma cells resistant to cisplatin. *Cancer Lett.*, **144**, 39–43.
25. Volate, S.R. *et al.* (2005) Modulation of aberrant crypt foci and apoptosis by dietary herbal supplements (quercetin, curcumin, silymarin, ginseng and rutin). *Carcinogenesis*, **26**, 1450–1456.
26. Park, S. *et al.* (2007) Inhibitory activities and attenuated expressions of 5-LOX with red ginseng in *Helicobacter pylori*-infected gastric epithelial cells. *Dig. Dis. Sci.*, **52**, 973–982.
27. Oh, G.S. *et al.* (2004) 20(S)-Protopanaxatriol, one of ginsenoside metabolites, inhibits inducible nitric oxide synthase and cyclooxygenase-2 expressions through inactivation of nuclear factor-kappaB in RAW 264.7 macrophages stimulated with lipopolysaccharide. *Cancer Lett.*, **205**, 23–29.
28. Behrens, J. (2000) Control of beta-catenin signaling in tumor development. *Ann. N. Y. Acad. Sci.*, **910**, 21–33; discussion 33–35.
29. Weiss, C. *et al.* (2004) Deregulated repression of c-Jun provides a potential link to its role in tumorigenesis. *Cell Cycle*, **3**, 111–113.
30. Eferl, R. *et al.* (2003) Liver tumor development. c-Jun antagonizes the proapoptotic activity of p53. *Cell*, **112**, 181–192.
31. Dressler, G.R. *et al.* (1992) Pax-2 is a DNA-binding protein expressed in embryonic kidney and Wilms tumor. *Proc. Natl Acad. Sci. USA*, **89**, 1179–1183.
32. Muratovska, A. *et al.* (2003) Paired-Box genes are frequently expressed in cancer and often required for cancer cell survival. *Oncogene*, **22**, 7989–7997.
33. Busse, A. *et al.* (2009) An intron 9 containing splice variant of PAX2. *J. Transl. Med.*, **7**, 36.
34. Wu, W.K. *et al.* (2009) Expression of ErbB receptors and their cognate ligands in gastric and colon cancer cell lines. *Anticancer Res.*, **29**, 229–234.
35. Ross, J.S. (2009) Breast cancer biomarkers and HER2 testing after 10 years of anti-HER2 therapy. *Drug News Perspect.*, **22**, 93–106.
36. Kuremsky, J.G. *et al.* (2009) Biomarkers for response to neoadjuvant chemoradiation for rectal cancer. *Int. J. Radiat. Oncol. Biol. Phys.*, **74**, 673–688.
37. Baron, A.T. *et al.* (2009) Clinical implementation of soluble EGFR (sEGFR) as a therapeutic serum biomarker of breast, lung and ovarian cancer. *IDrugs*, **12**, 302–308.
38. Shen, L. *et al.* (2008) EGFR and HER2 expression in primary cervical cancers and corresponding lymph node metastases: implications for targeted radiotherapy. *BMC Cancer*, **8**, 232.
39. Yamaoka, T. *et al.* (2008) Transactivation of EGF receptor and ErbB2 protects intestinal epithelial cells from TNF-induced apoptosis. *Proc. Natl Acad. Sci. USA*, **105**, 11772–11777.
40. Pi, X. *et al.* (2004) Big mitogen-activated protein kinase (BMK1)/ERK5 protects endothelial cells from apoptosis. *Circ. Res.*, **94**, 362–369.
41. Akao, Y. *et al.* (2009) Role of microRNA-143 in Fas-mediated apoptosis in human T-cell leukemia Jurkat cells. *Leuk. Res.*, **20**, 20.
42. Guo, Y.S. *et al.* (2002) Gastrin stimulates cyclooxygenase-2 expression in intestinal epithelial cells through multiple signaling pathways. Evidence for involvement of ERK5 kinase and transactivation of the epidermal growth factor receptor. *J. Biol. Chem.*, **277**, 48755–48763.
43. Yoo, J. *et al.* (2009) Protein kinase D mediates synergistic expression of COX-2 induced by TNF- α and bradykinin in human colonic myofibroblasts. *Am. J. Physiol. Cell Physiol.*, **297**, C1576–C1587.
44. Trauzold, A. *et al.* (2003) PKC μ prevents CD95-mediated apoptosis and enhances proliferation in pancreatic tumour cells. *Oncogene*, **22**, 8939–8947.
45. Kusunoki, M. *et al.* (1992) Protein kinase C activity in human colonic adenoma and colorectal carcinoma. *Cancer*, **69**, 24–30.
46. Wali, R.K. *et al.* (1995) Mechanism of action of chemoprotective ursodeoxycholate in the azoxymethane model of rat colonic carcinogenesis: potential roles of protein kinase C- α , - β II, and - ζ . *Cancer Res.*, **55**, 5257–5264.
47. Ozawa, F. *et al.* (2000) Enhanced expression of Silencer of death domains (SODD/BAG-4) in pancreatic cancer. *Biochem. Biophys. Res. Commun.*, **271**, 409–413.
48. Takada, H. *et al.* (2003) Role of SODD in regulation of tumor necrosis factor responses. *Mol. Cell. Biol.*, **23**, 4026–4033.
49. Lania, A.G. *et al.* (2004) Proliferation of transformed somatotroph cells related to low or absent expression of protein kinase a regulatory subunit 1A protein. *Cancer Res.*, **64**, 9193–9198.
50. Mantovani, G. *et al.* (2008) Different expression of protein kinase A (PKA) regulatory subunits in cortisol-secreting adrenocortical tumors: relationship with cell proliferation. *Exp. Cell Res.*, **314**, 123–130.
51. Farrow, B. *et al.* (2003) Inhibition of pancreatic cancer cell growth and induction of apoptosis with novel therapies directed against protein kinase A. *Surgery*, **134**, 197–205.
52. Whitesell, L. *et al.* (1994) Inhibition of heat shock protein HSP90-pp60v-src heteroprotein complex formation by benzoquinone ansamycins: essential role for stress proteins in oncogenic transformation. *Proc. Natl Acad. Sci. USA*, **91**, 8324–8328.
53. Banerji, U. (2009) Heat shock protein 90 as a drug target: some like it hot. *Clin. Cancer Res.*, **15**, 9–14.
54. Lundgren, K. *et al.* (2009) BIIB021, an orally available, fully synthetic small-molecule inhibitor of the heat shock protein Hsp90. *Mol. Cancer Ther.*, **8**, 921–929.
55. Smith, N.F. *et al.* (2006) Preclinical pharmacokinetics and metabolism of a novel diaryl pyrazole resorcinol series of heat shock protein 90 inhibitors. *Mol. Cancer Ther.*, **5**, 1628–1637.
56. McDonald, E. *et al.* (2006) Inhibitors of the HSP90 molecular chaperone: attacking the master regulator in cancer. *Curr. Top Med. Chem.*, **6**, 1091–1107.
57. Nosh, K. *et al.* (2006) Overexpression of poly(ADP-ribose) polymerase-1 (PARP-1) in the early stage of colorectal carcinogenesis. *Eur. J. Cancer*, **42**, 2374–2381.
58. Li, M. *et al.* (2009) Poly(ADP-ribose) polymerase inhibition down-regulates expression of metastasis-related genes in CT26 colon carcinoma cells. *Pathobiology*, **76**, 108–116.
59. Ratnam, K. *et al.* (2007) Current development of clinical inhibitors of poly(ADP-ribose) polymerase in oncology. *Clin. Cancer Res.*, **13**, 1383–1388.
60. Gottipati, S. *et al.* (2008) IRAK1: a critical signaling mediator of innate immunity. *Cell Signal.*, **20**, 269–276.
61. Fujiki, H. *et al.* (2009) Carcinogenic aspects of protein phosphatase 1 and 2A inhibitors. *Prog. Mol. Subcell. Biol.*, **46**, 221–254.
62. Douglas, P. *et al.* (2010) Protein phosphatase 6 interacts with the DNA-dependent protein kinase catalytic subunit and dephosphorylates gamma-H2AX. *Mol. Cell. Biol.*, **30**, 1368–1381.
63. Lemieux, E. *et al.* (2009) Constitutively active MEK1 is sufficient to induce epithelial-to-mesenchymal transition in intestinal epithelial cells and to promote tumor invasion and metastasis. *Int. J. Cancer*, **125**, 1575–1586.
64. Hersey, P. *et al.* (2009) Small molecules and targeted therapies in distant metastatic disease. *Ann. Oncol.*, **20**, vi35–vi40.
65. Sachdev, D. *et al.* (2007) Disrupting insulin-like growth factor signaling as a potential cancer therapy. *Mol. Cancer Ther.*, **6**, 1–12.
66. Frasca, F. *et al.* (2008) The role of insulin receptors and IGF-I receptors in cancer and other diseases. *Arch. Physiol. Biochem.*, **114**, 23–37.
67. Kamradt, M.C. *et al.* (2001) The small heat shock protein alpha B-crystallin negatively regulates cytochrome c- and caspase-8-dependent activation of caspase-3 by inhibiting its autoproteolytic maturation. *J. Biol. Chem.*, **276**, 16059–16063.
68. Kamradt, M.C. *et al.* (2005) The small heat shock protein alpha B-crystallin is a novel inhibitor of TRAIL-induced apoptosis that suppresses the activation of caspase-3. *J. Biol. Chem.*, **280**, 11059–11066.
69. Mao, Y.W. *et al.* (2004) Human alphaA- and alphaB-crystallins bind to Bax and Bcl-X(S) to sequester their translocation during staurosporine-induced apoptosis. *Cell Death Differ.*, **11**, 512–526.
70. Liu, S. *et al.* (2007) Small heat shock protein alphaB-crystallin binds to p53 to sequester its translocation to mitochondria during hydrogen peroxide-induced apoptosis. *Biochem. Biophys. Res. Commun.*, **354**, 109–114.
71. Klemenz, R. *et al.* (1993) Expression of the murine small heat shock proteins hsp 25 and alpha B crystallin in the absence of stress. *J. Cell Biol.*, **120**, 639–645.
72. Weekes, J. *et al.* (2009) Irinotecan and colorectal cancer: the role of p53, VEGF-C and alpha-B-crystallin expression. *Int. J. Colorectal Dis.*, **10**, 10.
73. Even, Y. *et al.* (2006) CDC2L5, a Cdk-like kinase with RS domain, interacts with the ASF/SF2-associated protein p32 and affects splicing *in vivo*. *J. Cell. Biochem.*, **99**, 890–904.
74. Hook, S.S. *et al.* (2001) Ca(2+)-CaM-dependent kinases: from activation to function. *Annu. Rev. Pharmacol. Toxicol.*, **41**, 471–505.
75. Takai, N. *et al.* (2009) Targeting calcium/calmodulin-dependence kinase I and II as a potential anti-proliferation remedy for endometrial carcinomas. *Cancer Lett.*, **277**, 235–243.
76. Smith, J.A. *et al.* (2005) Identification of the first specific inhibitor of p90 ribosomal S6 kinase (RSK) reveals an unexpected role for RSK in cancer cell proliferation. *Cancer Res.*, **65**, 1027–1034.
77. Lee, K.W. *et al.* (2008) Enzastaurin, a protein kinase C beta inhibitor, suppresses signaling through the ribosomal S6 kinase and bad pathways and induces apoptosis in human gastric cancer cells. *Cancer Res.*, **68**, 1916–1926.

Received May 17, 2010; revised July 28, 2010; accepted July 30, 2010